

Draft, April 25, 2018

Edinburgh Preprint: 95/555
 Granada Preprint UG-DFM-3/96
 Marseille CPT-95/PE.3244
 Southampton Preprint SHEP-95/31

Heavy Baryon Spectroscopy from the Lattice

UKQCD Collaboration

K.C. Bowler, R.D. Kenway, O. Oliveira, D.G. Richards, P. Ueberholz¹

Department of Physics & Astronomy, The University of Edinburgh, Edinburgh EH9 3JZ,
 Scotland

L. Lellouch², **J. Nieves**³, **C.T. Sachrajda**⁴, **N. Stella, H. Wittig**⁵

Physics Department, The University, Southampton SO17 1BJ, UK

Abstract

The results of an exploratory lattice study of heavy baryon spectroscopy are presented. We have computed the full spectrum of the eight baryons containing a single heavy quark, on a $24^3 \times 48$ lattice at $\beta = 6.2$, using an $O(a)$ -improved fermion action. We discuss the lattice baryon operators and give a method for isolating the contributions of the spin doublets (Σ, Σ^*) , (Ξ', Ξ^*) and (Ω, Ω^*) to the correlation function of the relevant operator. We compare our results with the available experimental data and find good agreement in both the charm and the beauty sectors, despite the long extrapolation in the heavy quark mass needed in the latter case. We also predict the masses of several undiscovered baryons. We compute the Λ – pseudoscalar meson and Σ – Λ mass splittings. Our results, which have errors in the range 10 – 30%, are in good agreement with the experimental numbers. For the $\Sigma^* - \Sigma$ mass splitting, we

¹Present address: Department of Physics, University of Wuppertal, Wuppertal D-42097, Germany

²Permanent address: Centre de Physique Théorique, CNRS Luminy, Case 907, F-13288 Marseille Cedex 9, France.

³Permanent address: Departamento de Física Moderna, Universidad de Granada, 18071, Spain.

⁴Address from 1 Oct. 1995 to 1 Oct. 1996: Theory Division, CERN, 1211 Geneva 23, Switzerland.

⁵Present address: DESY-IFH, Platanenallee 6, D-15738 Zeuthen, Germany

find results considerably smaller than the experimental values for both the charm and the beauty baryons, although in the latter case the experimental results are still preliminary. This is also the case for the lattice results for the hyperfine splitting for the heavy mesons.

1 Introduction

The discovery of the Λ_b baryon at LEP [1] and the claims of indirect evidence for Λ_b and Ξ_b semileptonic decays [2], have triggered an increased interest in the spectroscopy and weak decays of heavy baryons. The interest in the spectroscopy, in particular, has been considerably boosted after the announcement of the discovery of several spin- $\frac{3}{2}$ charm and beauty baryons [3, 4].

The properties of hadrons containing a heavy quark can be studied using lattice QCD calculations, which provide non-perturbative, model-independent results. Experience gained through studies of heavy mesons has provided the framework for an investigation of the phenomenology of heavy baryons. Furthermore, the study of the spectrum of heavy baryons is a necessary precondition for the measurement of the weak matrix elements of semileptonic decays of beauty baryons. The computed masses and matrix elements can then be combined with an analysis carried out in Heavy Quark Effective Theory (HQET) [5, 6] to extract an independent measurement of the CKM matrix elements V_{cb} and V_{ub} .

The subject of spectroscopy has been widely discussed in the literature, mainly using potential models [7], HQET [8], or a combination of the latter with chiral perturbation theory [9]. Recently, there have been attempts to compute the mass of the Λ_h (one heavy quark and two light quarks) [10] and of the Ξ_{hh} (two heavy quarks and one light quark) on the lattice [11]. In this paper, for the first time, the full spectrum of the lowest-lying baryons containing one heavy quark is computed. In particular, we define operators suitable for the simulation of baryon spin doublets with total spin $\frac{1}{2}$ and $\frac{3}{2}$, like the (Σ, Σ^*) , (Ξ', Ξ^*) and (Ω, Ω^*) . The quality of the signal we have observed and the agreement of our estimates with the available experimental data are good, thus giving us confidence in the reliability of our predictions.

The quark content and quantum numbers of the baryons we have considered are summarised in Table 1. On the lattices available at present, it is not possible to simulate directly the beauty quark, whose mass is larger than the cutoff. Therefore we have computed four heavy quark masses around that of the charm quark and interpolated (extrapolated) the results to the charm (beauty) quark, relying on the predictions of HQET. The masses of the charm and beauty quark were fixed from the masses of the D and B mesons, respectively. The results of the extrapolation in the heavy quark mass, could be checked carefully, given the relatively large sample of masses available. On the other hand, we have only used two different values of the light quark mass, thus limiting our ability to perform a detailed analysis of the chiral behaviour. Our results for the masses are given in Table 2, where the first set of errors is purely statistical and the second set is an estimate of the systematic uncertainty in the calibration of the lattice spacing. Our results are in good agreement with the experimental

determinations, where available¹. We also present estimates for the $\Lambda -$ pseudoscalar meson mass splittings. Our results are

$$\frac{M_{\Lambda_c} - M_D}{M_{\Lambda_c} + M_D} = 0.099^{+9}_{-7} \quad \frac{M_{\Lambda_b} - M_B}{M_{\Lambda_b} + M_B} = 0.033^{+5}_{-4} \quad (1)$$

to be compared with the experimental values²

$$\frac{M_{\Lambda_c} - M_D}{M_{\Lambda_c} + M_D} = 0.100(3) \quad \frac{M_{\Lambda_b} - M_B}{M_{\Lambda_b} + M_B} = 0.033(5). \quad (2)$$

Similarly, for the $\Sigma - \Lambda$ splitting, we find

$$\frac{M_{\Sigma_c} - M_{\Lambda_c}}{M_{\Sigma_c} + M_{\Lambda_c}} = 0.039^{+9}_{-9} \quad \frac{M_{\Sigma_b} - M_{\Lambda_b}}{M_{\Sigma_b} + M_{\Lambda_b}} = 0.017^{+5}_{-7} \quad (3)$$

which compares well with the experimental numbers

$$\frac{M_{\Sigma_c} - M_{\Lambda_c}}{M_{\Sigma_c} + M_{\Lambda_c}} = 0.035(1) \quad \frac{M_{\Sigma_b} - M_{\Lambda_b}}{M_{\Sigma_b} + M_{\Lambda_b}} = 0.016(2). \quad (4)$$

The last number in Eq. (4), extracted from the data presented in ref. [4], is still preliminary.

We also make a first attempt to estimate the spin splitting of the doublets (Σ^*, Σ) , (Ξ^*, Ξ') and (Ω^*, Ω) by isolating the contributions which the two particles give to the same correlation function. We find small, negative splittings, which, in most cases, become compatible with zero after the extrapolations because of the increased statistical errors. The simple quark model expectation is that the splittings are positive, although some of the experimental data are still inconclusive. If this expectation is confirmed by experiment, we could be facing a situation similar to that of the hyperfine splitting in heavy meson systems, where the splitting is underestimated using both the standard Wilson action and the Sheikholeslami-Wohlert (SW) action [14]. The meson hyperfine splitting is sensitive to the chromomagnetic moment term which appears at $O(a)$ in improved fermion actions [15]. We plan to investigate the sensitivity of the baryon hyperfine splitting by using the tadpole-improved Sheikholeslami-Wohlert action [16].

This paper is organised as follows: in Section 2 we discuss the baryonic operators which have been used in the present study and give details of the simulation. In Section 3 we explain our analysis procedures for the extraction of the masses. The measurement of the mass splittings is reported in Section 4. Our results and the comparison with the physical values are reported in Section 5. Finally, we present our conclusions.

¹The experimental evidence for the Ξ'_c baryon is based on a collection of 11 events, and no estimate of the statistical error is given, see ref. [12]. We note that the physical Ξ'_h and Ξ_h states are mixtures of the states which we measure here, where the light-quark system has definite spin. It has been argued that such mixing [13] becomes negligible in the heavy quark limit [8, 9]. See the conclusions for further comments.

² Errors on the experimental data are added in quadrature.

Baryon	(S)	J^P	(I)	$s_l^{\pi_l}$	Quark Content	Operator
$\Lambda_{c,b}$	(0)	$\frac{1}{2}^+$	(0)	0^+	$(ud)c, b$	\mathcal{O}_5
$\Sigma_{c,b}$	(0)	$\frac{1}{2}^+$	(1)	1^+	$(uu)c, b$	\mathcal{O}_μ
$\Sigma_{c,b}^*$	(0)	$\frac{3}{2}^+$	(1)	1^+	$(uu)c, b$	\mathcal{O}_μ
$\Xi_{c,b}$	(-1)	$\frac{1}{2}^+$	($\frac{1}{2}$)	0^+	$(us)c, b$	\mathcal{O}_5
$\Xi'_{c,b}$	(-1)	$\frac{1}{2}^+$	($\frac{1}{2}$)	1^+	$(us)c, b$	\mathcal{O}'_μ
$\Xi^*_{c,b}$	(-1)	$\frac{3}{2}^+$	($\frac{1}{2}$)	1^+	$(us)c, b$	\mathcal{O}'_μ
$\Omega_{c,b}$	(-2)	$\frac{1}{2}^+$	(0)	1^+	$(ss)c, b$	\mathcal{O}_μ
$\Omega^*_{c,b}$	(-2)	$\frac{3}{2}^+$	(0)	1^+	$(ss)c, b$	\mathcal{O}_μ

Table 1: Summary of the quantum numbers of the eight baryons containing a single heavy quark. I , $s_l^{\pi_l}$ are the isospin and the spin-parity of the light degrees of freedom and S , J^P are the strangeness and the spin-parity of the baryon.

2 Particles and Operators

There are eight lowest-lying baryons containing one heavy and two light quarks (up, down or strange). The quantum numbers of the charm and beauty baryons are listed in Table 1, and their physical masses (see refs. [3, 4, 17, 18]), are given in Table 2. In the context of HQET at lowest order, it is possible to identify the spin-parity quantum numbers of the heavy quark and of the light system, within each baryon. Furthermore, heavy baryons with common light degrees of freedom exhibit common features; they are expected to be degenerate in mass, and to obey selection rules in weak decays. For example, the hyperfine mass splittings in the doublets (Σ^*, Σ) , (Ξ^*, Ξ') and (Ω^*, Ω) are expected to be $O(1/m_h)$, where m_h is the mass of the heavy quark, and the weak semileptonic decay $\Lambda_b \rightarrow \Sigma_c$ is suppressed since it could only take place if the light quark system changed quantum numbers.

2.1 Operators for Heavy Baryons

The spectrum of the heavy baryons in Table 1 can be computed on the lattice by using the following three interpolating operators:

$$\mathcal{O}_5 = \epsilon_{abc}(l^{aT}\mathcal{C}\gamma_5 l^b)h^c; \quad \mathcal{O}_\mu = \epsilon_{abc}(l^{aT}\mathcal{C}\gamma_\mu l^b)h^c; \quad \mathcal{O}'_\mu = \epsilon_{abc}(l^{aT}\mathcal{C}\gamma_\mu l^b)h^c \quad (5)$$

where a, b, c are colour indices, ϵ_{abc} is the totally antisymmetric Levi-Civita tensor, \mathcal{C} is the charge conjugation matrix, l, l' are light quark fields, and h is the heavy-quark field. The (implicit) spinorial index of the three operators, is the (implicit) uncontracted Dirac index carried by the heavy quark field. By employing the operators in Eq. (5), one creates

Baryon	Quark Content	$h = \textit{charm}$		$h = \textit{beauty}$	
		Exp. [MeV]	Latt. [GeV]	Exp. [MeV]	Latt. [GeV]
Λ_h	$(ud)h$	2285(1)	2.27 ^{+4 +3} _{-3 -3}	5641(50)	5.64 ^{+5 +3} _{-5 -2}
Σ_h	$(uu)h$	2453(1)	2.46 ^{+7 +5} _{-3 -5}	5814(60)	5.77 ^{+6 +4} _{-6 -4}
Σ_h^*	$(uu)h$	2530(7)	2.44 ^{+6 +4} _{-4 -5}	5870(60)	5.78 ^{+5 +4} _{-6 -3}
Ξ_h	$(us)h$	2468(4)	2.41 ^{+3 +4} _{-3 -4}		5.76 ^{+3 +4} _{-5 -3}
Ξ_h'	$(us)h$	2560 [†]	2.57 ^{+6 +6} _{-3 -6}		5.90 ^{+6 +4} _{-6 -4}
Ξ_h^*	$(us)h$	2643(2)	2.55 ^{+5 +6} _{-4 -5}		5.90 ^{+4 +4} _{-6 -5}
Ω_h	$(ss)h$	2704(20)	2.68 ^{+5 +5} _{-4 -6}		5.99 ^{+5 +5} _{-5 -5}
Ω_h^*	$(ss)h$		2.66 ^{+5 +6} _{-3 -7}		6.00 ^{+4 +5} _{-5 -5}

Table 2: *Heavy baryons considered in this project. Our results are quoted with a statistical error (first) and a systematic error (second) arising from the uncertainty in the calibration of the lattice spacing. Where available, we report the experimental data.*

([†] For the error on the Ξ_c' mass, see footnote 1.)

physical states whose heavy quark and light quark systems have definite quantum numbers, corresponding to the HQET description at lowest order.

The operator \mathcal{O}_5 corresponds to $s_l^{\pi l} = 0^+$ spin-parity for the light degrees of freedom and a total spin-parity for the baryon $J^P = \frac{1}{2}^+$. The total isospin of the light degrees of freedom is $I = 0$ if $l = u$ and $l' = d$, and $I = \frac{1}{2}$ if one of the light quarks is the strange quark.

Consider the two-point correlation function G_5 :

$$G_5(\vec{p}, t) = \sum_{\vec{x}} e^{-i\vec{p}\cdot\vec{x}} \langle \mathcal{O}_5(\vec{x}, t) \overline{\mathcal{O}}_5(\vec{0}, 0) \rangle. \quad (6)$$

For large time separations, using antiperiodic boundary conditions in the time direction, this becomes in the continuum limit

$$G_5(\vec{p}, t) \rightarrow \frac{Z^2}{2E} \{e^{-Et}(M + \not{p}) - e^{-E(T-t)}(M - \not{p})\} + \frac{Z_{PP}^2}{2E_{PP}} \{e^{-E_{PP}t}(M_{PP} - \not{q}) - e^{-E_{PP}(T-t)}(\tilde{q} + M_{PP})\} \quad (7)$$

where $p^\mu = (E, \vec{p})$ is the 4-momentum of the baryon and $\tilde{p}^\mu = (E, -\vec{p})$. In Eq. (7), we have included the contribution of the parity partner (PP) baryon, with 4-momentum $q^\mu = (E_{PP}, \vec{p})$ and $\tilde{q}^\mu = (E_{PP}, -\vec{p})$. This particle contributes to the correlation function because it has a non-zero overlap with the operator \mathcal{O}_5 given in Eq. (5). At zero momentum, we choose

an appropriate combination of spinorial indices such that the baryon, but not the parity partner, propagates forward in time. We find that the amplitude of the parity partner (Z_{PP}^2) propagating backward in time is much smaller than that of the forward-propagating baryon (Z^2), and, in the following, we will neglect the contribution of the parity partners.

The case of the operator \mathcal{O}_μ is more involved than that of \mathcal{O}_5 since it transforms reducibly under the parity extended Lorentz group. It is the tensor product of a four vector and a Dirac spinor and thus transforms as $(1, \frac{1}{2}) \oplus (\frac{1}{2}, 1) \oplus (\frac{1}{2}, 0) \oplus (0, \frac{1}{2})$ (in $SU(2) \otimes SU(2)$ notation). It can annihilate/create particles of spin-parity $\frac{3}{2}^+$ and $\frac{1}{2}^+$ as well as these particles' parity partners. With the two-point function for the operator \mathcal{O}_μ defined as

$$G_{\mu\nu}(\vec{p}, t) = \sum_{\vec{x}} e^{-i\vec{p}\cdot\vec{x}} \langle \mathcal{O}_\mu(\vec{x}, t) \overline{\mathcal{O}}_\nu(\vec{0}, 0) \rangle, \quad (8)$$

we find, in the continuum limit, for large values of t and using antiperiodic boundary conditions in time,

$$\begin{aligned} G_{\mu\nu}(\vec{p}, t) \rightarrow & \frac{Z_{3/2}^2}{2E_{3/2}} e^{-E_{3/2}t} (\not{P}_{3/2} + M_{3/2})(P^{3/2})_{\mu\nu}(p_{3/2}) \\ & + \frac{e^{-E_{1/2}t}}{2E_{1/2}} \left\{ Z_1^2 (\not{P}_{1/2} + M_{1/2})(P_{11}^{1/2})_{\mu\nu}(p_{1/2}) - Z_2^2 (\not{P}_{1/2} - M_{1/2})(P_{22}^{1/2})_{\mu\nu}(p_{1/2}) \right. \\ & \left. - Z_1 Z_2 (\not{P}_{1/2} + M_{1/2})(P_{12}^{1/2})_{\mu\nu}(p_{1/2}) + Z_2 Z_1 (\not{P}_{1/2} - M_{1/2})(P_{21}^{1/2})_{\mu\nu}(p_{1/2}) \right\} \\ & + \text{parity partners} - \text{antiparticles} , \end{aligned} \quad (9)$$

where $p_J^\mu = (E_J, \vec{p})$ and where parity partner contributions are obtained from the original particle contributions with the replacement $M_J \rightarrow -M_{PP,J}$ while antiparticle contributions are obtained from the original particle and parity partner contributions with the replacement $M \rightarrow -M$, $\vec{p} \rightarrow -\vec{p}$ and $t \rightarrow T - t$ in the exponent. For any given momentum p_μ , the quantities $(P^{3/2})_{\mu\nu}(p)$ and $(P_{ij}^{1/2})_{\mu\nu}(p)$, $i, j = 1, 2$, are the spin projection operators of ref. [19] and are given by

$$\begin{aligned} (P^{3/2})_{\mu\nu}(p) &= g_{\mu\nu} - \frac{1}{3}\gamma_\mu\gamma_\nu - \frac{1}{3p^2}(\not{P}\gamma_\mu p_\nu + p_\mu\gamma_\nu\not{P}) , \\ (P_{11}^{1/2})_{\mu\nu}(p) &= \frac{1}{3}\gamma_\mu\gamma_\nu - \frac{1}{p^2}p_\mu p_\nu + \frac{1}{3p^2}(\not{P}\gamma_\mu p_\nu + p_\mu\gamma_\nu\not{P}) , \\ (P_{22}^{1/2})_{\mu\nu}(p) &= \frac{1}{p^2}p_\mu p_\nu , \\ (P_{12}^{1/2})_{\mu\nu}(p) &= \frac{1}{\sqrt{3}p^2}(p_\mu p_\nu - \not{P}\gamma_\mu p_\nu) \\ (P_{21}^{1/2})_{\mu\nu}(p) &= \frac{1}{\sqrt{3}p^2}(\not{P}p_\mu\gamma_\nu - p_\mu p_\nu) . \end{aligned} \quad (10)$$

They are orthonormal and idempotent

$$(P_{ij}^I)_{\mu\rho}(P_{kl}^J)^{\rho\nu} = \delta^{IJ}\delta_{jk}(P_{il}^J)_{\mu}^{\nu} \quad (11)$$

where I, J take on values $\frac{1}{2}$ or $\frac{3}{2}$. They satisfy

$$\begin{aligned}\gamma_\mu(P^{3/2})^\mu_\nu &= 0 ; & p_\mu(P^{3/2})^{\mu\nu} &= 0 = (P^{3/2})^{\mu\nu} p_\nu ; \\ p_\mu(P_{1j}^{1/2})^{\mu\nu} &= 0 = (P_{i1}^{1/2})^{\mu\nu} p_\nu & \text{for } i, j = 1, 2\end{aligned}\tag{12}$$

and have the following useful properties

$$\begin{aligned}\not{p}(P_{ij}^{1/2})^{\mu\nu} &= \pm(P_{ij}^{1/2})^{\mu\nu}\not{p} \quad + \text{for } i = j, - \text{for } i \neq j \\ \not{p}(P^{3/2})^{\mu\nu} &= (P^{3/2})^{\mu\nu}\not{p}.\end{aligned}\tag{13}$$

The properties of Eqs. (12) and (13) guarantee that the spin- $\frac{3}{2}$ contribution satisfies the appropriate Rarita-Schwinger equations [20] and that the spin- $\frac{1}{2}$ contributions satisfy the appropriate Dirac equations. The diagonal projectors are furthermore complete:

$$g_{\mu\nu} = (P^{3/2})_{\mu\nu}(p) + (P_{11}^{1/2})_{\mu\nu}(p) + (P_{22}^{1/2})_{\mu\nu}(p) .\tag{14}$$

To extract the masses of the spin-parity $\frac{1}{2}^+$ and $\frac{3}{2}^+$ particles, one needs only to compute the correlators (9) at rest. In this case, the projectors $P^{3/2}$ and $P_{11}^{1/2}$ simplify to

$$\begin{aligned}(P^{3/2})^{ij} &= g^{ij} - \frac{1}{3}\gamma^i\gamma^j; \quad i, j = 1, 2, 3, \\ (P_{11}^{1/2})^{ij} &= \frac{1}{3}\gamma^i\gamma^j,\end{aligned}\tag{15}$$

and only act on the spatial components of $G_{\mu\nu}(\vec{0}, t)$, i.e. $\mu, \nu = 1, 2, 3$. Since the components corresponding to the other projection operators do not contribute to the spatial components, $G_{ij}(\vec{0}, t)$, it is clear from the properties of $P^{3/2}$ and $P_{11}^{1/2}$ given in Eqs. (11) and (13) that the $\frac{3}{2}^+$ contribution can be isolated by considering $(P^{3/2})^{ij}G_{jk}(\vec{0}, t)$ and the $\frac{1}{2}^+$ contribution, by considering $(P_{11}^{1/2})^{ij}G_{jk}(\vec{0}, t)$. The contributions of forward-propagating parity partners are suppressed by taking suitable combinations of spinorial indices as discussed after Eq. (7) for the case of $G_5(\vec{0}, t)$. Those of the backward-propagating parity partners are naturally smaller because the time intervals over which they propagate are much longer for most values of t that we consider in analysing $G_{jk}(\vec{0}, t)$. Furthermore, both contributions are again empirically found to be suppressed by the fact that the overlaps of the parity partner states with the operator \mathcal{O}^μ are orders of magnitude smaller and their masses slightly larger than those of the original particles.

When space-time is approximated by a hypercubic lattice, full Euclidean $O(4)$ symmetry is reduced to symmetry under the hypercubic group. This reduction means that most irreducible representations of $O(4)$ and its covering group become reducible on the lattice. Fortunately, the representations which concern us here, $(1, \frac{1}{2})$, $(\frac{1}{2}, 1)$, $(\frac{1}{2}, 0)$ and $(0, \frac{1}{2})$, because of their low dimensionality, remain irreducible on the lattice [35]. Furthermore, when restricted to the diagonal cubic subgroup (i.e. the lattice analogue of the rotation subgroup),

$(1, \frac{1}{2}) \oplus (\frac{1}{2}, 1)$ decomposes into the reducible representation $\frac{3}{2} \oplus \frac{1}{2}$ while $(\frac{1}{2}, 0) \oplus (0, \frac{1}{2})$ reduces to $\frac{1}{2}$, where $\frac{1}{2}$ and $\frac{3}{2}$ are themselves reductions to the cubic group of continuum spin- $\frac{1}{2}$ and spin- $\frac{3}{2}$ representations. Thus, the space-time transformation properties of the operators \mathcal{O}_5 and \mathcal{O}_μ on the lattice are analogous to what they are in the continuum. Moreover, using the results of Ref. [35], one can show that the cubic representations $\frac{1}{2}$ and $\frac{3}{2}$ mix only with the following continuum spins:

$$\left(\frac{1}{2}\right)_{\text{cubic}} : \frac{1}{2}, \frac{7}{2}, \frac{9}{2}, \dots \quad \left(\frac{3}{2}\right)_{\text{cubic}} : \frac{3}{2}, \frac{5}{2}, \frac{7}{2}, \dots \quad (16)$$

Therefore, if one isolates correctly the cubic $\frac{1}{2}$ and $\frac{3}{2}$ contributions to $G_{\mu\nu}(\vec{p}, t)$, one isolates unambiguously the contributions of the continuum spin- $\frac{1}{2}$ and spin- $\frac{3}{2}$ states in the large time limit (assuming, of course, that higher spin states are more massive). It should be emphasized that this isolation of the cubic representations must be done carefully because it is not known, a priori, which of the spin- $\frac{1}{2}$ or the spin- $\frac{3}{2}$ states is more massive. Fortunately, at zero momentum the continuum rest frame projectors given in Eq. (15) are sufficient because they implement the Clebsch-Gordan decomposition of the product representation $\text{spin-}1 \otimes \text{spin-}\frac{1}{2}$ into $\text{spin-}\frac{1}{2}$ and $\text{spin-}\frac{3}{2}$, a decomposition which survives the reduction of $SU(2)$ to the double valued cubic subgroup because irreducible representations of $SU(2)$ with spin less than or equal to $\frac{3}{2}$ are irreducible when reduced to that subgroup. It should further be noted that properties of operators and states under parity transformations are unaffected by the discretization of space-time.

A similar discussion applies to the operator \mathcal{O}'_μ . In fact, the structure of the corresponding correlator in terms of quark propagators is the same as that of \mathcal{O}_μ ; the only effect of the additional Wick contraction in the \mathcal{O}_μ correlator is to change the overall normalization.

Thus we have shown in the present section how to isolate the contributions of the different physical baryon states to the two-point functions of Eqs. (7) and (9). In the following sections we shall use these procedures to determine the heavy-light baryon spectrum. To improve the overlap of the interpolating operators \mathcal{O}_5 , \mathcal{O}_μ and \mathcal{O}'_μ with the corresponding physical baryon states, we smear these operators as described in the Appendix. Though this smearing further complicates the isolation of the various physical baryon state contributions for non-zero two-point function momentum \vec{p} (please refer to the Appendix for details), the baryon spectrum that we obtain here only requires an analysis of zero-momentum, smeared two-point functions to which the discussion of the present section applies unchanged.

2.2 Details of the Simulation

Our calculation is performed on 60 $SU(3)$ gauge field configurations generated on a $24^3 \times 48$ lattice at $\beta = 6.2$, using the hybrid over-relaxed algorithm described in ref. [22]. The quark

propagators were computed using the $O(a)$ -improved Sheikholeslami-Wohlert action, which is related to the standard Wilson fermion action via

$$S_F^{SW} = S_F^W - i\frac{\kappa}{2} \sum_{x,\mu,\nu} \bar{q}(x) F_{\mu\nu}(x) \sigma_{\mu\nu} q(x), \quad (17)$$

where κ is the hopping parameter. The use of the SW action reduces discretisation errors from $O(ma)$ to $O(\alpha_s ma)$ [23, 24], which is of particular importance in our study of heavy baryons, where the bare heavy quark masses are typically around one third to two thirds of the inverse lattice spacing.

The gauge field configurations and light quark propagators were generated on the 64-node i860 Meiko Computing Surface at the University of Edinburgh. The heavy quark propagators were computed using the 256-node Cray T3D, also at Edinburgh.

Statistical errors are calculated according to the bootstrap procedure described in [22], for which the quoted errors on all quantities correspond to 68% confidence limits of the distribution obtained from 1000 bootstrap samples.

In order to convert our values for baryon masses and mass splittings into physical units we need an estimate of the inverse lattice spacing in GeV. In this study we take

$$a^{-1} = 2.9 \pm 0.2 \text{ GeV}, \quad (18)$$

thus deviating slightly from some of our earlier papers, where we quoted 2.7 GeV as the central value [22, 25, 34]. The error in equation (18) is large enough to encompass all our estimates for a^{-1} from quantities such as m_ρ , f_π , m_N , the string tension \sqrt{K} and the hadronic scale R_0 discussed in [27]. This change is partly motivated by a recent study using newly generated UKQCD data [28]; using the quantity R_0 we found $a^{-1} = 2.95^{+7}_{-11}$ GeV. Also, the non-perturbative determination of the renormalisation constant of the axial current yielded a value of $Z_A = 1.05(1)$ [29] which is larger by about 8% than the perturbative value which we used previously. Thus the scale estimated from f_π decreases to around 3.1 GeV which enables us to reduce significantly the upper uncertainty on our final value of a^{-1} [GeV].

Light quark propagators were computed for quark masses around the strange quark mass, corresponding to hopping parameters $\kappa = 0.14144$ and 0.14226 . Because each heavy baryon contains two light quarks, we can form three baryon correlators for each heavy quark mass, of which two have degenerate light-quark masses and one has non-degenerate light-quark masses. The masses of the light pseudoscalar meson which are needed for this study, were obtained in ref. [25]. Results extrapolated to the chiral limit (corresponding to a hopping parameter $\kappa_{\text{crit}} = 0.14315^{+2}_{-2}$) and to the mass of the strange quark ($\kappa_s = 0.1419^{+1}_{-1}$) are also tabulated there.

The heavy quark propagators have been computed for four values of the heavy quark mass around that of the charm quark, corresponding to $\kappa_h = 0.133, 0.129, 0.125$ and 0.121 . The

masses of the heavy-light pseudoscalar mesons can be found in ref. [34].

In order to enhance the signal for the baryon correlation functions, the light and heavy quark propagators have been computed using the Jacobi smearing method [30], either at the source only (SL) or at both the source and the sink (SS). Since smearing is not a Lorentz-invariant operation, it might alter some of the transformation properties of non-scalar observables. We have found that such an effect is evident in the baryonic correlators at non-zero momentum, and we present the results of a study of these effects in Appendix A. This issue, which does not affect the spectrum, represents an important new effect which is crucial in the extraction of the amplitude Z , and therefore in the measurement of the weak matrix elements entering the semileptonic decays of the Λ_b .

3 Analysis Details

It follows from Eq. (7), that, for $t > 0$

$$[G_5(\vec{0}, t)]_{11} = [G_5(\vec{0}, t)]_{22} = -[G_5(\vec{0}, T - t)]_{33} = -[G_5(\vec{0}, T - t)]_{44}. \quad (19)$$

Therefore, we define the Λ correlation function as ³:

$$G_\Lambda(t) = \frac{1}{4} \left[[G_5(\vec{0}, t)]_{11} + [G_5(\vec{0}, t)]_{22} - [G_5(\vec{0}, T - t)]_{33} - [G_5(\vec{0}, T - t)]_{44} \right] \simeq Z_\Lambda^2 e^{-m_\Lambda t} \quad (20)$$

Similarly, for the Σ and Σ^* , we define the correlation functions by taking suitable combinations of the equivalent components, after projection with the operators given in Eq. (15).

3.1 The Effective Masses

In Fig. 1 we show effective mass plots of the Λ and Σ baryons, in both the SL and SS cases. We compute the effective masses assuming that the correlators' time evolution is given by an exponential:

$$M_{\text{eff}}(t) = \ln \left(\frac{G_{\Lambda, \Sigma}(t)}{G_{\Lambda, \Sigma}(t + 1)} \right). \quad (21)$$

This is justified since we have checked that the contribution of the parity partners propagating backward in time is completely negligible.

The effective mass is smoother for SL than for SS correlators, because the former are more correlated in time. To establish a fitting range, we fitted the correlators to a single exponential in the range $[t_{\text{min}}, t_{\text{max}}]$, where t_{max} was fixed at 21 for SS and 23 for SL correlators,

³ Λ is a conventional name, by which we mean the baryon whose light quarks are in a $s^\pi = 0^+$ state. Depending on the flavour of the latter, this baryon is either the physical $\Lambda(ud)$ or the $\Xi(us)$ with spin 0 for the light quarks. A similar convention is used for Σ and Σ^* .

and t_{\min} was varied between 8 and 19. The fits at fixed values of the light and heavy kappas were obtained by minimizing the χ^2 computed using the full covariance matrix.

As an example, we show in Fig. 2 the results of this analysis for both the Λ and the Σ , with $\kappa_h = 0.129$ and $\kappa_{l1} = \kappa_{l2} = 0.14144$, for both SS and SL correlators. The behaviour of the correlator for the Σ^* baryon is similar, and the features described below are common to all the masses considered in this study.

By considering the χ^2/dof of the fits, as well as the stability of the results under variation of t_{\min} , we make the following observations:

1. The masses obtained from the fits to the SS correlators are stable and the χ^2/dof are acceptable for $t_{\min} \geq 11$. For the SL correlators, the χ^2/dof are acceptable only for $t_{\min} \geq 16$. This behaviour supports the hypothesis that by smearing both the sink and the source one enhances the overlap with the ground state.
2. The masses obtained from fits to the SL and SS correlators agree around $t_{\min} \geq 17$
3. As a general feature, we observe that the statistical errors increase with decreasing light quark mass. This effect is more pronounced for SL than for SS correlators.

The conclusion is that there is good agreement between SS and SL data, even if, in the latter cases, the plateaux are shorter and the errors slightly larger. Thus we quote the results obtained by fitting SS correlators in $t \in [12, 21]$, using those obtained with SL correlators as a consistency check.

3.2 Mass Extrapolations

We obtain the masses of the eight charm and beauty baryons by extrapolating first in the light quark masses and then in the heavy quark mass.

3.2.1 Extrapolation in the Light Quark Mass

In order to perform the extrapolation to the chiral limit, we use the three baryon masses obtained from both degenerate (i.e. $\kappa_{l1} = \kappa_{l2} = 0.14144$, or 0.14226) and non-degenerate (i.e. $\kappa_{l1} = 0.14144$ and $\kappa_{l2} = 0.14226$) light quark correlation functions. We assume that, in the chiral regime, M_{baryon} depends linearly on the sum of the two light quark masses, that is,

$$\begin{aligned}
 M_{\text{baryon}}(\kappa_h, \kappa_{l1}, \kappa_{l2}) &= M_{\text{baryon}}(\kappa_h) + C \left(\frac{1}{2\kappa_{l1}} + \frac{1}{2\kappa_{l2}} - \frac{1}{\kappa_{\text{crit}}} \right) \\
 &= M_{\text{baryon}}(\kappa_h) + C \left(\frac{1}{\kappa_{\text{eff}}} - \frac{1}{\kappa_{\text{crit}}} \right)
 \end{aligned} \tag{22}$$

with $\kappa_{\text{eff}}^{-1} = (\kappa_{l1}^{-1} + \kappa_{l2}^{-1})/2$. This is supported by our data for the masses in the Λ and Σ channels, as shown in Fig. 3, and by previous studies of light meson masses [25, 26]. In the Λ channel, extrapolating to $\kappa_{l1} = \kappa_{l2} = \kappa_{\text{crit}}$ gives the mass of the Λ_h , while extrapolating κ_{l1} to κ_{crit} and interpolating κ_{l2} to κ_s gives the mass of the Ξ_h . Similarly, from the Σ channel we extract the masses of the Σ_h , the Ξ'_h and the Ω_h .

The results of this analysis, obtained from SS correlation functions, are summarised in Table 3. By performing the same type of analysis on the SL correlators, we obtained essentially indistinguishable results. We note that the difference in the statistical errors of the SS and SL masses, already present in the fits at fixed κ , is amplified by the extrapolation to the chiral limit. This confirms our earlier conclusion that by using SS data one obtains more precise results.

3.3 Heavy Quark Extrapolation

The physical masses of the charmed and beauty baryons are obtained by extrapolating the four sets of data, computed at $\kappa_h = 0.133, 0.129, 0.125$ and 0.121 . In performing these extrapolations, we have been guided by the HQET and have expressed the dependence of the baryon mass $M_{\text{baryon}}(M_P)$ on the heavy-light pseudoscalar meson mass, M_P , through the following function

$$M_{\text{baryon}}(M_P) = M_P + C + \frac{A}{M_P} \quad (23)$$

where the two constants C and A are the parameters of the fit. The masses of the charm and beauty baryons are obtained for $M_P = M_D$ or $M_P = M_B$ respectively. In Table 2 we report the results, corresponding to the SS case, in physical units. The numbers corresponding to the charm and beauty masses have been obtained assuming $a^{-1} = 2.9$ GeV. The quoted systematic error arises solely from the uncertainty in the scale and has been estimated by letting a^{-1} vary by one standard deviation about its central value.

In these fits, the coefficient A , which quantifies the size of the $1/m_h$ corrections, is of the expected size, i.e. $A = O(\Lambda_{\text{QCD}}^2)$, ranging from about $(350\text{MeV})^2$ to $(540\text{MeV})^2$, depending on the particular baryon and on the flavour of the light degrees of freedom. Of course, the $O(1/m_h)$ corrections play an important role in the case of the mass splittings, (see section 4), while they contribute much less to the value of each mass. As a further confirmation of this, we have also set A to zero and verified that the results of the extrapolation are essentially indistinguishable from those presented in Table 2 although the χ^2 are significantly higher. Finally we have used a function of the kind

$$M_{\text{baryon}}(M_P) = C + A'(M_P - M_0) \quad (24)$$

where a different slope in M_P is allowed, and we have obtained A' compatible with 1 in most cases. All of this confirms that heavy quark symmetry is very well satisfied here. Moreover

Λ :	κ_l	$\kappa_h = 0.121$	$\kappa_h = 0.125$	$\kappa_h = 0.129$	$\kappa_h = 0.133$
	0.14144/0.14144	1.138 $^{+8}_{-7}$	1.040 $^{+9}_{-5}$	0.939 $^{+9}_{-4}$	0.829 $^{+9}_{-4}$
	0.14144/0.14226	1.108 $^{+11}_{-6}$	1.011 $^{+11}_{-5}$	0.908 $^{+11}_{-4}$	0.798 $^{+11}_{-4}$
	0.14226/0.14226	1.077 $^{+11}_{-7}$	0.979 $^{+12}_{-6}$	0.875 $^{+12}_{-5}$	0.764 $^{+12}_{-5}$
	strange/strange	1.101 $^{+13}_{-9}$	1.002 $^{+13}_{-9}$	0.899 $^{+13}_{-9}$	0.786 $^{+13}_{-9}$
	strange/chiral	1.056 $^{+14}_{-9}$	0.959 $^{+15}_{-7}$	0.853 $^{+14}_{-6}$	0.740 $^{+14}_{-7}$
	chiral/chiral	1.011 $^{+17}_{-13}$	0.913 $^{+16}_{-11}$	0.807 $^{+15}_{-10}$	0.693 $^{+14}_{-10}$
χ_{dof}^2	0.05	0.3	0.2	0.9	
Σ :	κ_l	$\kappa_h = 0.121$	$\kappa_h = 0.125$	$\kappa_h = 0.129$	$\kappa_h = 0.133$
	0.14144/0.14144	1.176 $^{+12}_{-7}$	1.078 $^{+13}_{-6}$	0.977 $^{+14}_{-6}$	0.869 $^{+14}_{-6}$
	0.14144/0.14226	1.150 $^{+15}_{-7}$	1.053 $^{+15}_{-7}$	0.950 $^{+17}_{-7}$	0.842 $^{+18}_{-7}$
	0.14226/0.14226	1.126 $^{+18}_{-9}$	1.030 $^{+18}_{-9}$	0.927 $^{+19}_{-9}$	0.818 $^{+21}_{-8}$
	strange/strange	1.141 $^{+18}_{-11}$	1.043 $^{+18}_{-10}$	0.941 $^{+18}_{-11}$	0.833 $^{+18}_{-11}$
	strange/chiral	1.108 $^{+22}_{-10}$	1.010 $^{+22}_{-11}$	0.908 $^{+23}_{-10}$	0.801 $^{+25}_{-10}$
	chiral/chiral	1.067 $^{+23}_{-23}$	0.965 $^{+23}_{-12}$	0.862 $^{+23}_{-10}$	0.753 $^{+23}_{-13}$
χ_{dof}^2	0.8	0.1	1.0	0.7	
Σ^* :	κ_l	$\kappa_h = 0.121$	$\kappa_h = 0.125$	$\kappa_h = 0.129$	$\kappa_h = 0.133$
	0.14144/0.14144	1.170 $^{+11}_{-7}$	1.072 $^{+12}_{-7}$	0.969 $^{+12}_{-6}$	0.860 $^{+12}_{-6}$
	0.14144/0.14226	1.145 $^{+13}_{-8}$	1.047 $^{+13}_{-8}$	0.944 $^{+14}_{-7}$	0.834 $^{+14}_{-7}$
	0.14226/0.14226	1.121 $^{+15}_{-9}$	1.023 $^{+15}_{-9}$	0.920 $^{+16}_{-9}$	0.809 $^{+17}_{-8}$
	strange/strange	1.136 $^{+16}_{-10}$	1.038 $^{+16}_{-10}$	0.934 $^{+16}_{-9}$	0.823 $^{+17}_{-9}$
	strange/chiral	1.104 $^{+18}_{-11}$	1.005 $^{+18}_{-10}$	0.902 $^{+19}_{-10}$	0.791 $^{+20}_{-9}$
	chiral/chiral	1.061 $^{+22}_{-13}$	0.960 $^{+22}_{-12}$	0.856 $^{+22}_{-11}$	0.745 $^{+22}_{-10}$
χ_{dof}^2	0.4	0.7	0.6	0.5	

Table 3: Masses of the Λ , Σ and Σ^* in lattice units obtained by fitting the SS correlators in $t \in [12, 21]$. Also shown are the corresponding masses after extrapolation in the light-quark masses, using Eq. 22.

the insensitivity of the results to the different modelling functions gives us confidence, not only in the interpolation to the charm mass, but also in the long extrapolation to the beauty mass. We stress, once more, the total agreement between SS and SL results, both for the final numbers and the features of the extrapolations. Two examples of the extrapolation to the heavy scale, corresponding to the Λ and the Σ are shown in Figs. 4.

4 Calculation of mass splittings

Once the value of κ_h is fixed to correspond to the physical quark mass by matching M_P to either the D - or the B -meson mass, no large uncertainties are expected to occur in the measurement of other charm or beauty hadron masses, which are largely determined by that of the heavy quark. On the other hand, splittings in the masses arise from the dynamics of the light quarks and their interactions with the heavy quark. Their study provides a test of HQET as well as important information on the size of various systematic effects.

The mass splittings are small quantities in comparison to the baryon masses themselves. Thus, they are affected by relatively larger statistical errors, as well as being more sensitive to the fitting and extrapolation procedures adopted. Therefore, a particularly careful analysis is required. Once more, we will quote results obtained by fitting SS correlators; the SL correlators give consistent results, although the statistical errors are appreciably larger.

4.1 Λ –Pseudoscalar Meson Mass Splitting

The Λ – pseudoscalar meson mass splitting is very precisely measured experimentally, especially in the charm sector. Therefore, as we use the pseudoscalar mass to fix the value of the heavy quark κ , the agreement of the lattice value of $M_\Lambda - M_P$ with experiment reflects the extent to which our calculation properly incorporates the dynamics of the light degrees of freedom. The amount of computational effort devoted to this calculation, both with static [31]-[33] and propagating Wilson fermions [11] is testimony to its importance. We summarize the results obtained so far [32, 33] and compare them with the numbers from this study in Fig. 5.

For the analysis of this splitting we need the correlation function of the pseudoscalar meson, which was determined in an earlier simulation [34] using the same heavy quarks as this study, but with one additional light quark, corresponding to $\kappa_l = 0.14262$. We find that there is very little to be gained by determining the difference of the masses from the time evolution of the ratio of the Λ and the pseudoscalar meson correlators⁴, as opposed to obtaining it

⁴Since the behaviour of the baryon and meson time slice correlators is different close to the centre of the lattice, the ratio method is only safe if one excludes the last few timeslices from the fitting range.

κ_{l1}/κ_{l2}	$\kappa_h = 0.121$	$\kappa_h = 0.125$	$\kappa_h = 0.129$	$\kappa_h = 0.133$
0.14144/0.14144	0.212 $^{+7}_{-8}$	0.216 $^{+8}_{-6}$	0.222 $^{+8}_{-5}$	0.229 $^{+8}_{-4}$
0.14226/0.14226	0.173 $^{+10}_{-10}$	0.178 $^{+10}_{-8}$	0.182 $^{+10}_{-7}$	0.189 $^{+10}_{-6}$
<i>chiral/chiral</i>	0.131 $^{+15}_{-15}$	0.138 $^{+15}_{-12}$	0.140 $^{+14}_{-11}$	0.145 $^{+14}_{-10}$

Table 4: Λ -pseudoscalar meson mass splitting, in lattice units, obtained from the difference of the fitted masses.

by subtracting the two masses determined separately. One reason is that the statistical errors associated with our measurement of the Λ mass are much larger than those of the pseudoscalar, and would dominate the final uncertainty on the splitting in any procedure. Moreover, when the pseudoscalar correlators were computed, only the heavy quark propagators were smeared. Here the light quark propagators are also smeared, and consequently the pseudoscalar and baryon correlation functions suffer from different statistical fluctuations. Therefore, we measure the splitting by taking the difference of the baryon mass, obtained as described in the previous section, and the meson mass, fitted in the range $t \in [12, 21]$, as in ref. [34]. The results, for all the kappa values, are reported in Table 4.

We perform a chiral extrapolation of the mass differences at each heavy κ value. Although we have simulated only two values of the light quark mass we have computed baryon correlators corresponding to two degenerate and one non-degenerate case; this last set of data, however, cannot be matched with the mesonic data and cannot be used in the chiral extrapolation. Hence, the chiral extrapolation is modelled by a linear function of the two degenerate light-quark points. Both our results for the Λ extrapolation (see section 3) and the evidence reported in ref. [25] for the meson, justify this procedure.

We performed the extrapolation to the physical pseudoscalar meson masses following two different procedures, in order to have a consistency check (see figure 6).

- A** The splittings are first extrapolated in the inverse heavy quark mass, according to the formula

$$\left[M_\Lambda - M_P \right](\kappa_h) = A + \frac{B}{M_P(\kappa_h)} + \frac{C}{M_P^2(\kappa_h)},$$

keeping the light quark mass fixed. The linear and quadratic extrapolations produce indistinguishable numbers. Then the two values of this splitting corresponding to the two degenerate light-quark configurations are extrapolated to the chiral limit for each heavy-quark mass.

- B** We employ the reverse procedure in which the mass splittings are first extrapolated to

	procedure A [MeV]	procedure B [MeV]	experiment [MeV]
charm	406 $^{+44}_{-29}$	408 $^{+41}_{-31}$	415(1)
beauty	354 $^{+55}_{-46}$	359 $^{+55}_{-45}$	362(50)

Table 5: *Results for the $\Lambda -$ pseudoscalar splitting, at the physical masses, corresponding to $a^{-1} = 2.9 \text{ GeV}$. The two methods illustrated in the text produce essentially identical results, in excellent agreement with the experimental number, given in the last column.*

the chiral limit, keeping the heavy quark mass fixed. The results from the subsequent linear and quadratic extrapolations in the heavy quark mass are once again compatible.

We conclude that the behaviour of the Λ -pseudoscalar splitting is well represented by a linear function of both the light quark mass and the inverse heavy quark mass. The results in physical units that we quote in Table 5 are obtained under this assumption.

4.2 $\Sigma - \Lambda$ Mass Splitting

We have obtained the $\Sigma - \Lambda$ mass splitting for the various κ combinations, both by taking the difference of the fitted masses and by fitting the time evolution of the ratio of Σ and Λ correlators. The numbers obtained with the two methods are in good agreement, but the second procedure yields appreciably smaller errors and is smoother in the chiral limit, proving that it is particularly appropriate when one compares two correlators with a similar structure. The results at each value of the computed masses and after the chiral extrapolation are given in Table 6.

The dependence of the splitting on the heavy quark mass is extremely weak, suggesting that the $1/m_h$ corrections to the masses of the two baryons must be very similar and nearly cancel in the difference. This feature makes it particularly simple to perform the extrapolation to the physical masses, as the fits to linear and quadratic functions of the inverse pseudoscalar meson mass are essentially indistinguishable. This is clearly visible in Fig. 7. We note that our results, presented in Table 7, compare very well with experiment.

4.3 Spin Splitting

In the HQET, the mass difference within the spin doublets (Σ, Σ^*) , (Ξ', Ξ^*) and (Ω, Ω^*) is due to the coupling of the chromomagnetic moment of the heavy quark to the light degrees of freedom. It is therefore suppressed by inverse powers of the heavy-quark mass and vanishes in the infinite mass limit.

κ_{l1}/κ_{l2}	$\kappa_h = 0.121$	$\kappa_h = 0.125$	$\kappa_h = 0.129$	$\kappa_h = 0.133$
0.14144/0.14144	$(0.37 \begin{smallmatrix} +6 \\ -4 \end{smallmatrix}) \times 10^{-1}$	$(0.36 \begin{smallmatrix} +7 \\ -4 \end{smallmatrix}) \times 10^{-1}$	$(0.37 \begin{smallmatrix} +7 \\ -4 \end{smallmatrix}) \times 10^{-1}$	$(0.37 \begin{smallmatrix} +6 \\ -4 \end{smallmatrix}) \times 10^{-1}$
0.14144/0.14226	$(0.44 \begin{smallmatrix} +7 \\ -8 \end{smallmatrix}) \times 10^{-1}$	$(0.44 \begin{smallmatrix} +8 \\ -7 \end{smallmatrix}) \times 10^{-1}$	$(0.43 \begin{smallmatrix} +8 \\ -7 \end{smallmatrix}) \times 10^{-1}$	$(0.44 \begin{smallmatrix} +8 \\ -6 \end{smallmatrix}) \times 10^{-1}$
0.14226/0.14226	$(0.50 \begin{smallmatrix} +12 \\ -11 \end{smallmatrix}) \times 10^{-1}$	$(0.49 \begin{smallmatrix} +12 \\ -10 \end{smallmatrix}) \times 10^{-1}$	$(0.52 \begin{smallmatrix} +10 \\ -11 \end{smallmatrix}) \times 10^{-1}$	$(0.51 \begin{smallmatrix} +11 \\ -8 \end{smallmatrix}) \times 10^{-1}$
<i>chiral/strange</i>	$(0.54 \begin{smallmatrix} +15 \\ -15 \end{smallmatrix}) \times 10^{-1}$	$(0.50 \begin{smallmatrix} +17 \\ -13 \end{smallmatrix}) \times 10^{-1}$	$(0.59 \begin{smallmatrix} +13 \\ -15 \end{smallmatrix}) \times 10^{-1}$	$(0.57 \begin{smallmatrix} +14 \\ -10 \end{smallmatrix}) \times 10^{-1}$
<i>chiral/chiral</i>	$(0.65 \begin{smallmatrix} +17 \\ -18 \end{smallmatrix}) \times 10^{-1}$	$(0.65 \begin{smallmatrix} +18 \\ -18 \end{smallmatrix}) \times 10^{-1}$	$(0.67 \begin{smallmatrix} +17 \\ -17 \end{smallmatrix}) \times 10^{-1}$	$(0.66 \begin{smallmatrix} +17 \\ -14 \end{smallmatrix}) \times 10^{-1}$

Table 6: *Estimates of $M_\Sigma - M_\Lambda$ in lattice units, for the various kappa combinations, obtained with the ratio method. The extrapolations are linear, as they were for the masses themselves.*

Because the splitting is such a small number, it is difficult to measure from our data using either the ratio of the correlators or the difference of the fitted masses. We find that the difference of the masses gives smoother chiral behaviour, and so we obtain our estimates using this method.

We present our measurements of the splittings for each κ combination in Table 8 and the extrapolated values at the physical masses in Table 7. They are negative within two standard deviations at fixed light-quark mass, but being affected by large statistical errors, become compatible with zero in the chiral limit. We obtain the splittings at the physical masses, extrapolating in the inverse heavy-quark mass, according to the following function

$$\left[M_{\Sigma^*} - M_\Sigma \right](\kappa_h) = \frac{A}{M_P(\kappa_h)} + \frac{B}{M_P^2(\kappa_h)}. \quad (25)$$

The splitting has been constrained to vanish in the infinite heavy-quark mass limit, as predicted by the HQET. The two extrapolations obtained either by including the quadratic term or by setting $B = 0$ gave essentially indistinguishable results, as can be seen from Fig. 8, and good χ^2 . We also checked the consistency of our data with the predicted behaviour, by adding a constant to the function (25), i.e. by allowing the spin-splitting to have a non-zero intercept, at $1/M_P = 0$. We find that the values of the intercept are always compatible with zero, being of the order -30 MeV, with errors of about one hundred.

Once more, the results were perfectly consistent. The values presented in Table 7 correspond to Eq. (25), with $B = 0$ since this parametrization fits the lattice data very well and makes full use of heavy-quark scaling relations.

We note that our value for the $\Sigma_c^* - \Sigma_c$ splitting is inconsistent with experiment, and in most cases our measured values are consistent with zero. This feature resembles the well-known puzzle of the spin splitting in the mesonic sector [14], whose resolution is believed to lie in a combination of discretisation and quenching effects, as argued in ref. [15]. In the light of this,

	$h = \text{charm}$			$h = \text{beauty}$		
	Exp.	Latt.		Exp.	Latt.	
$\Lambda_h - P$	[18] 417(1)	408	$\begin{smallmatrix} +41 & +34 \\ -31 & -33 \end{smallmatrix}$	[18] 362(50)	359	$\begin{smallmatrix} +55 & +27 \\ -45 & -26 \end{smallmatrix}$
$\Sigma_h - \Lambda_h$	[18] 169(2)	190	$\begin{smallmatrix} +50 & +13 \\ -43 & -13 \end{smallmatrix}$	[4] 173(11)	190	$\begin{smallmatrix} +60 & +13 \\ -75 & -13 \end{smallmatrix}$
$\Xi'_h - \Xi_h$	[12] 92	166	$\begin{smallmatrix} +40 & +12 \\ -35 & -13 \end{smallmatrix}$		157	$\begin{smallmatrix} +52 & +11 \\ -64 & -11 \end{smallmatrix}$
$\Sigma_h^* - \Sigma_h$	[19] 77(6)	-17	$\begin{smallmatrix} +12 & +3 \\ -31 & -2 \end{smallmatrix}$	[4] 56(16)	-6	$\begin{smallmatrix} +4 & +1 \\ -11 & -1 \end{smallmatrix}$
$\Xi_h^* - \Xi'_h$	[12] 83	-20	$\begin{smallmatrix} +12 & +2 \\ -24 & -3 \end{smallmatrix}$		-7	$\begin{smallmatrix} +4 & +1 \\ -8 & -1 \end{smallmatrix}$
$\Omega_h^* - \Omega'_h$		-23	$\begin{smallmatrix} +6 & +3 \\ -14 & -2 \end{smallmatrix}$		-8	$\begin{smallmatrix} +2 & +1 \\ -5 & -1 \end{smallmatrix}$

Table 7: *Baryon-pseudoscalar meson and baryon-baryon mass splittings in MeV. The available experimental data are also shown, together with the corresponding references. The experimental errors on the $\Xi'_c - \Xi_c$ and $\Xi_c^* - \Xi'_c$ splittings are not published.*

and also considering the very large statistical errors, firm conclusion about the consistency of our results with heavy-quark scaling laws cannot be drawn.

5 Physical Results

In this section, we present a summary of the results obtained in this study, in a form which is easily comparable with the experimental data. All masses are given with an asymmetric statistical error arising from the bootstrap analysis, and a systematic error due solely to the uncertainty in the scale (see Eq. (18)).

In Table 2 we quote the charm and beauty baryon masses, together with the experimental values, where available. Our results agree well with the experimental data for the charm sector, and also for Λ_b and Σ_b , despite the long extrapolation in the heavy mass scale needed in these cases. This gives us confidence in the reliability of our predictions for the masses of the undiscovered charm and beauty baryons. The quality of the results at the beauty mass was certainly enhanced by the number of heavy quark masses available for this investigation, which allowed us to try different extrapolation procedures and to perform consistency checks. On the other hand, we only have a limited sample of light quark masses. Although the light extrapolations were always smooth and reasonable, the chiral behaviour should be confirmed by using a larger number of light quark masses.

We present the mass splittings of Section 4 in Table 7. In those cases where comparison with experiment is possible, we also compute the ratios of the splitting to the sum of the

κ_{l1}/κ_{l2}	$\kappa_h = 0.121$	$\kappa_h = 0.125$	$\kappa_h = 0.129$	$\kappa_h = 0.133$
0.14144/0.14144	$(-0.53^{+17}_{-28}) \times 10^{-2}$	$(-0.60^{+18}_{-30}) \times 10^{-2}$	$(-0.74^{+21}_{-34}) \times 10^{-2}$	$(-0.93^{+22}_{-41}) \times 10^{-2}$
0.14144/0.14226	$(-0.50^{+18}_{-39}) \times 10^{-2}$	$(-0.58^{+23}_{-42}) \times 10^{-2}$	$(-0.67^{+21}_{-49}) \times 10^{-2}$	$(-0.85^{+24}_{-58}) \times 10^{-2}$
0.14226/0.14226	$(-0.49^{+26}_{-57}) \times 10^{-2}$	$(-0.63^{+31}_{-62}) \times 10^{-2}$	$(-0.68^{+32}_{-68}) \times 10^{-2}$	$(-0.84^{+38}_{-78}) \times 10^{-2}$
<i>strange/strange</i>	$(-0.50^{+19}_{-41}) \times 10^{-2}$	$(-0.58^{+23}_{-43}) \times 10^{-2}$	$(-0.66^{+22}_{-52}) \times 10^{-2}$	$(-0.86^{+26}_{-61}) \times 10^{-2}$
<i>chiral/strange</i>	$(-0.40^{+36}_{-75}) \times 10^{-2}$	$(-0.50^{+45}_{-85}) \times 10^{-2}$	$(-0.63^{+48}_{-86}) \times 10^{-2}$	$(-0.97^{+56}_{-94}) \times 10^{-2}$
<i>chiral/chiral</i>	$(-0.42^{+41}_{-90}) \times 10^{-2}$	$(-0.55^{+48}_{-92}) \times 10^{-2}$	$(-0.43^{+40}_{-110}) \times 10^{-2}$	$(-0.64^{+49}_{-126}) \times 10^{-2}$

Table 8: *Estimates of $M_{\Sigma^*} - M_{\Sigma}$ in lattice units at the various masses, obtained by taking the difference of the fitted masses, in lattice units. The extrapolations are linear, following the same procedure adopted for the other splittings.*

masses, to eliminate most of the uncertainty in the scale. These results were presented in the Introduction, see Eqns (1-4). The residual systematic uncertainty, which is always smaller than the statistical error, was not quoted.

In those cases where a meaningful comparison with experiment is possible the agreement is very encouraging. Unfortunately, the mass differences, being small, are affected by large relative errors varying between 10 and 30%. Nevertheless, we stress the beautiful agreement with the experimental data, both at the charm and at the beauty mass. In particular, in our calculation of the $\Lambda_h -$ pseudoscalar meson splitting, the agreement with experiment has significantly improved on previous calculations, performed with the standard Wilson action. We believe that this success is further evidence of the advantages of using the Sheikholeslami-Wohlert fermion action.

6 Conclusions

In this paper we have presented the result of a lattice study of heavy baryon spectroscopy. The spectrum of the eight lowest-lying heavy baryons, containing a single heavy quark, can be computed using the three baryonic operators in Eq. (5). In addition to the calculation of the Λ and Ξ masses we have discussed how to compute the spectrum of the spin doublets, (Σ, Σ^*) , (Ξ', Ξ^*) and (Ω, Ω^*) , by isolating their contribution to the correlation functions of the operators \mathcal{O}_μ and \mathcal{O}'_μ .

The computation of the mass spectrum proved feasible; the operators we have used have a good overlap with the various baryon ground states, in part thanks to the smearing both at

the source and at the sink. Moreover, the extrapolations in both the heavy and light quark masses are always smooth. The agreement between our estimates of the baryon masses and the experimental values is good, in both the charm and the beauty sectors.

The computed Λ – pseudoscalar meson mass splitting is in good agreement with experiment, in contrast with the results of previous calculations performed with the Wilson fermion action. We believe that this is largely due to the use of the $O(a)$ -improved action to remove systematic effects. A similar positive conclusion can be drawn for the Σ – Λ splitting, although the statistical errors are still of the order of 25 – 30%.

Our results are also in agreement with the predictions obtained with other non-perturbative methods [7]-[9], both for the masses themselves and for the Σ – Λ splitting. In the case of the Ξ' – Ξ splitting, which is of the same nature as the Σ – Λ splitting, the calculation is complicated by the mixing arising between the two particles, whose total quantum numbers are the same. It has been noted [9] that such a mixing, negligible in the heavy quark limit, would have the effect of increasing the splitting. Both our prediction and that of Savage [9] are higher than experiment [12]. The disagreement would hence get even worse if we were to take the mixing into account. We stress, anyway, that this experimental result is still to be confirmed.

In this exploratory study the masses have been determined with reasonable precision, but further studies are required to reduce both the statistical and systematic errors. The results presented in this paper are very encouraging and it looks likely that it will also be possible to measure the baryonic matrix elements.

Acknowledgements The authors wish to thank Robert Coquereaux, Oleg Ogievetsky, Jay Watson and Jonathan Flynn for helpful discussions. This research was supported by the UK Science and Engineering Research Council under grants GR/G 32779, by the Particle Physics and Astronomy Research Council under grant GR/J 21347, by the European Union under contract CHRX-CT92-0051, by the University of Edinburgh and by Meiko Limited. CTS (Senior Fellow), and DGR (Advanced Fellow) acknowledge the support of the Particle Physics and Astronomy Research Council. NS thanks the University of Rome “La Sapienza” for financial support. JN and PU acknowledge the European Union for their support through the award of a Fellowship, contracts Nos. CHBICT920066 and CHBICT930877. OO is supported by JNICT under grant BD/2714/93.

A Effect of smearing on baryon correlation functions

In this appendix we propose a description of the effect of a non-Lorentz invariant smearing on a non-scalar operator. Interpolating operators are smeared to improve their overlap with the physical states one wishes to create or annihilate. We discuss the case of 2-point correlation functions, restricting ourselves to the case of spinorial operators which have overlap with a single type of spin 1/2 particle, like $\mathcal{O}_5(x)$ defined in Eqn. (5). Numerical evidence for this effect is also presented. It should be noted that the breaking of the Lorentz symmetry manifests itself only when one considers correlators at finite momentum, and has therefore no relevance to the determination of the spectrum.

Let us write the general expression for a local baryonic operator,

$$J_\rho(x) = \left(\psi(x)\Gamma\psi(x)\right)\psi_\rho(x), \quad (26)$$

and consider the case where it has overlap with spin 1/2 states, like \mathcal{O}_5 . It can destroy one such state, according to the relation

$$\langle 0|J_\rho(0)|\vec{p}, r\rangle = Zu_\rho^{(r)}(\vec{p}). \quad (27)$$

In Eqs. (26,27), ρ and r are the spinorial and polarization indices, respectively, the antisymmetric sum over colour is understood and Γ is a suitable combination of gamma and charge conjugation matrices. Finally, the amplitude Z is a Lorentz scalar.

In general, a smeared baryonic operator can be written as

$$J_\rho^s(\vec{x}, t) = \sum_{\vec{y}, \vec{z}, \vec{w}} f(|\vec{y} - \vec{x}|)f(|\vec{z} - \vec{x}|)f(|\vec{w} - \vec{x}|)\left(\psi(\vec{y}, t)\Gamma\psi(\vec{z}, t)\right)\psi_\rho(\vec{w}, t). \quad (28)$$

Because the smearing is performed only in the spatial directions, Lorentz symmetry is lost and only spatial translations, rotations, parity and time reversal survive. Therefore, the overlap of the operator $J_\rho^s(\vec{x}, t)$ with the state $|\vec{p}, r\rangle$ is given by the more general expression

$$\langle 0|J_\rho^s(0)|\vec{p}, r\rangle = \left[Z_1(|\vec{p}|)u^{(r)}(\vec{p}) + Z_2(|\vec{p}|)\gamma_0u^{(r)}(\vec{p})\right]_\rho \quad (29)$$

where the amplitudes Z_1 and Z_2 may depend on the magnitude of the three-momentum of the state $|\vec{p}, r\rangle$, in accord with the restricted symmetries of the system.

Let us consider the case of a SS two-point correlator, for large t

$$\begin{aligned} G_{\rho\sigma}^{ss}(t, \vec{p}) &= \sum_{\vec{x}} \langle 0|T[J_\rho^s(\vec{x}, t)\bar{J}_\sigma^s(\vec{0}, 0)]|0\rangle e^{-i\vec{p}\cdot\vec{x}} \\ &= \sum_{|\vec{q}, r} \sum_{\vec{x}} \frac{m}{E(\vec{p})} \langle 0|J_\rho^s(\vec{0}, 0)|\vec{q}, r\rangle \langle \vec{q}, r|\bar{J}_\sigma^s(\vec{0}, 0)|0\rangle e^{-i\vec{p}\cdot\vec{x}} e^{i\vec{q}\cdot\vec{x}} \\ &= \sum_r \frac{me^{-E(\vec{p})t}}{E(\vec{p})} \left[\left(Z_1(|\vec{p}|) + Z_2(|\vec{p}|)\gamma_0 \right) u^{(r)}(\vec{p}) \bar{u}^{(r)}(\vec{p}) \left(Z_1(|\vec{p}|) + Z_2(|\vec{p}|)\gamma_0 \right) \right]_{\rho\sigma}. \end{aligned} \quad (30)$$

This expression can be conveniently rewritten as

$$G_{\rho\sigma}^{ss}(t, \vec{p}) = Z_s^2(|\vec{p}|)e^{-E(\vec{p})t} \left[\frac{E + m - \alpha^2(E - m)}{4E} \mathbb{1} + \frac{E + m + \alpha^2(E - m)}{4E} \gamma_0 - \frac{2\alpha}{4E} \vec{p} \cdot \vec{\gamma} \right]_{\rho\sigma} \quad (31)$$

where $Z_s = Z_1 + Z_2$, $\alpha = (Z_1 - Z_2)/(Z_1 + Z_2)$ and full Lorentz symmetry is recovered when $\alpha = 1$. Eqn. (31) exhibits the following features:

- the exponential fall-off is not altered by the smearing. This was expected since a smearing function which only extends in the spatial directions preserves the form of the transfer matrix;
- it has the correct limit for $\alpha \rightarrow 1$: $G^{ss}(\vec{p}, t) \propto G^{\text{loc}}(\vec{p}, t)$;
- the degeneracy among the amplitudes of different spinorial components of the correlator is lifted;
- all the terms proportional to α vanish for $\vec{p} \rightarrow \vec{0}$, so that the effect disappears at zero momentum⁵.

In the following, we will check this effect against the numerical data. It is convenient to rewrite Eq. (31) in the form

$$G^{ss}(\vec{p}, t) = \frac{e^{-E(\vec{p})t}}{2E} \{mZ_m + \gamma_0 E Z_E - \vec{p} \cdot \vec{\gamma} Z_p\}, \quad \text{with} \quad \begin{cases} Z_E &= [E + m + \alpha^2(E - m)] \frac{Z_s^2}{2E} \\ Z_m &= [E + m - \alpha^2(E - m)] \frac{Z_s^2}{2m} \\ Z_p &= \alpha Z_s^2. \end{cases} \quad (32)$$

We have found that Z_E and Z_m are compatible, as they should be, considering that they differ by terms proportional to \vec{p}^2/Em , which are very small for the values of momenta and masses in our simulation. Furthermore Z_p is significantly different from Z_E and Z_m , which shows that α is different from one. Z_s and α are given by

$$Z_s^2 = \frac{EZ_E + mZ_m}{E + m} \quad \text{and} \quad \alpha = \frac{Z_p}{Z_s^2}. \quad (33)$$

The results of this exercise are presented in Table 9 for the Λ baryon with momentum $\vec{p} = (\frac{2\pi}{L}, 0, 0)$ and $(\frac{2\pi}{L}, \frac{2\pi}{L}, 0)$, for masses corresponding to the four values of κ_h and $\kappa_{l1} = \kappa_{l2} = 0.14144$. Using the estimated values of Z_s^2 and α we have also recomputed Z_E and Z_m (second row of Table 9) and verified that they are compatible with the fitted values. The numerical results are consistent with the picture illustrated above, and the value of α is significantly different from 1, demonstrating that such an effect cannot be neglected.

⁵For this reason, this effect has no consequences for the results presented in this paper.

$$\text{Momentum } \vec{p} = \left(\frac{2\pi}{L}, 0, 0 \right)$$

	Z_E^2	Z_m^2	Z_p^2	Z_s^2	α
$\kappa_h = 0.121$	$(2.84 \begin{smallmatrix} +40 \\ -37 \end{smallmatrix}) \times 10^4$	$(2.80 \begin{smallmatrix} +41 \\ -36 \end{smallmatrix}) \times 10^4$	$(1.86 \begin{smallmatrix} +17 \\ -14 \end{smallmatrix}) \times 10^4$	$(2.82 \begin{smallmatrix} +41 \\ -37 \end{smallmatrix}) \times 10^4$	$0.66 \begin{smallmatrix} +6 \\ -7 \end{smallmatrix}$
	$(2.80 \begin{smallmatrix} +40 \\ -36 \end{smallmatrix}) \times 10^4$	$(2.84 \begin{smallmatrix} +41 \\ -37 \end{smallmatrix}) \times 10^4$			
$\kappa_h = 0.125$	$(2.86 \begin{smallmatrix} +43 \\ -38 \end{smallmatrix}) \times 10^4$	$(2.79 \begin{smallmatrix} +44 \\ -37 \end{smallmatrix}) \times 10^4$	$(1.99 \begin{smallmatrix} +18 \\ -15 \end{smallmatrix}) \times 10^4$	$(2.83 \begin{smallmatrix} +44 \\ -38 \end{smallmatrix}) \times 10^4$	$0.71 \begin{smallmatrix} +7 \\ -7 \end{smallmatrix}$
	$(2.81 \begin{smallmatrix} +42 \\ -37 \end{smallmatrix}) \times 10^4$	$(2.85 \begin{smallmatrix} +44 \\ -38 \end{smallmatrix}) \times 10^4$			
$\kappa_h = 0.129$	$(2.83 \begin{smallmatrix} +35 \\ -30 \end{smallmatrix}) \times 10^4$	$(2.73 \begin{smallmatrix} +33 \\ -29 \end{smallmatrix}) \times 10^4$	$(2.17 \begin{smallmatrix} +20 \\ -17 \end{smallmatrix}) \times 10^4$	$(2.78 \begin{smallmatrix} +34 \\ -30 \end{smallmatrix}) \times 10^4$	$0.78 \begin{smallmatrix} +7 \\ -7 \end{smallmatrix}$
	$(2.76 \begin{smallmatrix} +34 \\ -29 \end{smallmatrix}) \times 10^4$	$(2.80 \begin{smallmatrix} + \\ - \end{smallmatrix}) \times 10^4$			
$\kappa_h = 0.133$	$(2.77 \begin{smallmatrix} +35 \\ -32 \end{smallmatrix}) \times 10^4$	$(2.62 \begin{smallmatrix} +34 \\ -29 \end{smallmatrix}) \times 10^4$	$(2.29 \begin{smallmatrix} +22 \\ -17 \end{smallmatrix}) \times 10^4$	$(2.69 \begin{smallmatrix} +36 \\ -30 \end{smallmatrix}) \times 10^4$	$0.85 \begin{smallmatrix} +8 \\ -7 \end{smallmatrix}$
	$(2.68 \begin{smallmatrix} +35 \\ -28 \end{smallmatrix}) \times 10^4$	$(2.71 \begin{smallmatrix} +36 \\ -32 \end{smallmatrix}) \times 10^4$			

$$\text{Momentum } \vec{p} = \left(\frac{2\pi}{L}, \frac{2\pi}{L}, 0 \right)$$

	Z_E^2	Z_m^2	Z_p^2	Z_s^2	α
$\kappa_h = 0.121$	$(1.94 \begin{smallmatrix} +28 \\ -35 \end{smallmatrix}) \times 10^4$	$(1.93 \begin{smallmatrix} +36 \\ -28 \end{smallmatrix}) \times 10^4$	$(1.09 \begin{smallmatrix} +14 \\ -11 \end{smallmatrix}) \times 10^4$	$(1.94 \begin{smallmatrix} +28 \\ -36 \end{smallmatrix}) \times 10^4$	$0.56 \begin{smallmatrix} +11 \\ -7 \end{smallmatrix}$
	$(1.90 \begin{smallmatrix} +27 \\ -35 \end{smallmatrix}) \times 10^4$	$(1.97 \begin{smallmatrix} +29 \\ -37 \end{smallmatrix}) \times 10^4$			
$\kappa_h = 0.125$	$(1.93 \begin{smallmatrix} +32 \\ -33 \end{smallmatrix}) \times 10^4$	$(1.91 \begin{smallmatrix} +32 \\ -33 \end{smallmatrix}) \times 10^4$	$(1.16 \begin{smallmatrix} +15 \\ -12 \end{smallmatrix}) \times 10^4$	$(1.92 \begin{smallmatrix} +32 \\ -33 \end{smallmatrix}) \times 10^4$	$0.61 \begin{smallmatrix} +12 \\ -8 \end{smallmatrix}$
	$(1.89 \begin{smallmatrix} +31 \\ -32 \end{smallmatrix}) \times 10^4$	$(1.96 \begin{smallmatrix} +32 \\ -34 \end{smallmatrix}) \times 10^4$			
$\kappa_h = 0.129$	$(1.93 \begin{smallmatrix} +32 \\ -33 \end{smallmatrix}) \times 10^4$	$(1.88 \begin{smallmatrix} +30 \\ -33 \end{smallmatrix}) \times 10^4$	$(1.25 \begin{smallmatrix} +16 \\ -13 \end{smallmatrix}) \times 10^4$	$(1.91 \begin{smallmatrix} +30 \\ -34 \end{smallmatrix}) \times 10^4$	$0.66 \begin{smallmatrix} +14 \\ -9 \end{smallmatrix}$
	$(1.87 \begin{smallmatrix} +29 \\ -31 \end{smallmatrix}) \times 10^4$	$(1.95 \begin{smallmatrix} +32 \\ -35 \end{smallmatrix}) \times 10^4$			
$\kappa_h = 0.133$	$(1.89 \begin{smallmatrix} +32 \\ -34 \end{smallmatrix}) \times 10^4$	$(1.79 \begin{smallmatrix} +32 \\ -32 \end{smallmatrix}) \times 10^4$	$(1.34 \begin{smallmatrix} +18 \\ -14 \end{smallmatrix}) \times 10^4$	$(1.84 \begin{smallmatrix} +32 \\ -33 \end{smallmatrix}) \times 10^4$	$0.73 \begin{smallmatrix} +16 \\ -10 \end{smallmatrix}$
	$(1.80 \begin{smallmatrix} +31 \\ -30 \end{smallmatrix}) \times 10^4$	$(1.88 \begin{smallmatrix} +34 \\ -36 \end{smallmatrix}) \times 10^4$			

Table 9: Estimates of α and Z_s^2 from the fitted values of Z_m, Z_E, Z_p . In the second row corresponding to each κ_h , the fitted Z_m and Z_E are compared with the estimates using Eq. (32), and the measured values of Z_s^2 and α .

We conclude this appendix with a discussion of the SL correlators, whose spin structure is again different from that of local correlators. This feature must be taken into account in the analysis of three-point correlators when the inserted current operator is local. Following the reasoning above, we find:

Momentum	$\kappa_h = 0.121$	$\kappa_h = 0.125$	$\kappa_h = 0.129$	$\kappa_h = 0.133$
$\vec{p} = \vec{0}$	$(3.8^{+4}_{-3}) \times 10^{-3}$	$(3.6^{+3}_{-3}) \times 10^{-3}$	$(3.5^{+3}_{-3}) \times 10^{-3}$	$(3.2^{+3}_{-2}) \times 10^{-3}$
$\vec{p} = (\frac{2\pi}{L}, 0, 0)$	$(3.9^{+4}_{-4}) \times 10^{-3}$	$(3.7^{+4}_{-4}) \times 10^{-3}$	$(3.6^{+4}_{-3}) \times 10^{-3}$	$(3.3^{+4}_{-3}) \times 10^{-3}$
$\vec{p} = (\frac{2\pi}{L}, \frac{2\pi}{L}, 0)$	$(3.8^{+5}_{-4}) \times 10^{-3}$	$(3.7^{+5}_{-4}) \times 10^{-3}$	$(3.5^{+5}_{-4}) \times 10^{-3}$	$(3.3^{+5}_{-4}) \times 10^{-3}$

Table 10: Values of $Z_l = (Z_l Z_s) / \sqrt{Z_s^2}$, for the four heavy masses and $\kappa_{l1} = \kappa_{l2} = 0.14144$.

$$G^{sl}(t, \vec{p}) = Z_l Z_s (|\vec{p}|) e^{-E(\vec{p})t} \left\{ \frac{E + m - \alpha(E - m)}{4E} \mathbb{I} + \frac{E + m + \alpha(E - m)}{4E} \gamma_0 - \frac{(1 + \gamma_0) + \alpha(1 - \gamma_0)}{4E} \vec{p} \cdot \vec{\gamma} \right\}. \quad (34)$$

As above, it is possible to measure $Z_s Z_l$ averaging Z_E and Z_m . By doing so, we have extracted Z_l for three different values of the momentum, and the results are shown in Table 10. The evidence that Z_l is independent of \vec{p} is a further check of the validity of our interpretation.

References

- [1] C. Albajar *et al.*, Phys. Lett. **B273**, (1991) 540;
G. Bari *et al.*, Nuovo Cimento **A104** (1991) 1787.
- [2] ALEPH Collaboration D. Decamp *et al.*, Phys. Lett. B **278**, 367 (1992);
OPAL Collaboration P. Acton *et al.*, Phys. Lett. B **281**, 394 (1992);
ALEPH Collaboration D. Buskulic. *et al.*, Phys. Lett. B **294**, 145 (1992);
DELPHI Collaboration P. Abreu *et al.*, Phys. Lett. B **311**, 379 (1993).
- [3] S. F. Biagi *et al.*, Zeit. Phys. C **28**, 175 (1985); ARGUS Collaboration, H. Albrecht *et al.*, Phys. Lett. B **288**, 367 (1992);
Fermilab E687 Collaboration, P. L. Frabetti *et al.*, Phys. Lett. B **300**, 190 (1993); **338**, 106 (1994); contribution to LISHEP95, Rio de Janeiro, February 1995;
CERN WA89 Collaboration, M. I. Adamovich *et al.*, Max-Planck-Institut report MPI-H-V27-1995, June, 1995, and references therein.
- [4] Several contributions at the EPS HEP-95 Conference focused on this topic. DELPHI Coll., DELPHI-95-107, Contribution # eps0565, Brussel, 1995.
- [5] For a review, see, e.g., M. Neubert; Heavy Quark Symmetry. Phys. Rept. **245** (1994) 245.
- [6] J.G. Körner, D. Pirjol and M. Krämer; Prog. Part. Nucl. Phys. **33** (1994) 787.

- [7] A. De Rújula, H. Georgi and S.L. Glashow. Phys. Rev. **D12** (1975) 147;
A. Martin and J.M. Richard; Phys. Lett.. **B185** (1987) 426,
and references therein.
- [8] J.L. Rosner, EFI-95-48, hep-lat/9508252;
R. Roncaglia, D.B. Lichtenberg and E. Predazzi. IU/NTC 95-03 hep-ph/9502251.
- [9] M.J. Savage, Report-no: CMU-HEP95-11, hep-ph/9508268; see also M.K. Banerjee and
J. Milana. Preprint DOE/ER/40762-051, UMPP #95-058, hep-ph/9410398.
- [10] UKQCD Collaboration (N. Stella) ; Nucl. Phys. B (Proc. Suppl.) **42** (1995) 367;
C. Alexandrou *et al.*, Nucl. Phys. B (Proc. Suppl.) **42** (1995) 297.
- [11] C. Alexandrou *et al.*, Phys. Lett. B **337**, 340 (1994).
- [12] WA89 Collaboration, P. Avery et al. CLNS 95/1352, CLEO 95-14, hep-ex/9508010.
- [13] J.L. Rosner, Prog. Theor. Phys. **66** (1981) 1422.
- [14] UKQCD Collaboration C.R. Allton *et al.*, Phys. Lett. B **292**, 408 (1992).
- [15] A.S. Kronfeld, P.B. Mackenzie. Ann. Rev. Nucl. Part. Sci. **43** (1993) 793, *and references
therein* .
- [16] G.P. Lepage and P.B. Mackenzie, Phys. Rev. D **48**, 2250 (1993).
UKQCD Collaboration, work in progress.
- [17] Particle Data Group, (L. Montanet et al.) Phys. Rev. D **50**, (1994).
- [18] SKAT Collaboration, V.V. Ammosov et al., paper #42 submitted to XVI International
Symposium on Lepton-Photon Intereactions, Cornell University, Ithaca (1993)
- [19] M. Benmerrouche *et al.*, Phys. Rev. C **39**, 2339 (1989).
- [20] W. Rarita and J. Schwinger. Phys. Rev. **60**, (1941) 61.
- [21] D. Luríe. Particles and Fields. Interscience Publishers, (1968).
- [22] UKQCD Collaboration, C.R. Allton *et al.*, Nucl. Phys. **B407**, 331 (1993).
- [23] B. Sheikholeslami and R. Wohlert, Nucl. Phys. **B259**, 572 (1985).
- [24] G. Heatlie, C.T. Sachrajda, G. Martinelli, C. Pittori and G.C. Rossi, Nucl. Phys. **B352**,
266 (1991).
- [25] UKQCD Collaboration, C.R. Allton *et al.*, Phys. Rev. D **49**, 474 (1994).

- [26] R. Gupta, to appear in the Proceedings of the Conference LATTICE95, Melbourne. hep-lat/9512021.
- [27] R. Sommer, Nucl. Phys. **B411**, 839 (1994); G. de Divitiis *et al.*, Nucl. Phys. **B437**, 447 (1994) .
- [28] UKQCD Collaboration (H. Wittig); Nucl. Phys. B (Proc. Suppl.) **42** (1995) 288.
- [29] UKQCD Collaboration, D.S. Henty *et al.*, Phys. Rev. D **51**, 5323 (1995).
- [30] UKQCD Collaboration, C.R. Allton *et al.*, Phys. Rev. D **47**, 5128 (1993).
- [31] M. Bochicchio, G. Martinelli, C.R. Allton, C.T. Sachrajda and D.B. Carpenter. Nucl. Phys. **B372**, 403 (1992).
- [32] UKQCD Collaboration (A.K. Ewing); Nucl. Phys. B (Prog. Suppl.) **B42** (1995) 331.
- [33] UKQCD Collaboration (A.K. Ewing *et al.*); Southampton preprint SHEP 95-20. hep-lat/9508030
- [34] UKQCD Collaboration, R.M. Baxter *et al.*, Phys. Rev. D **49**, 1594 (1994).
- [35] J.E. Mandula and E. Shpiz, Nucl. Phys. **B232**, 180 (1984).
- [36] L.C. Chen and J.L. Birman, J. Math. Phys. **12** (1971) 2454
- [37] J.E. Mandula, G. Zweig and J. Govaerts, Nucl. Phys. **B228**, 91 (1983) Nucl. Phys. **B228**, 109 (1983).

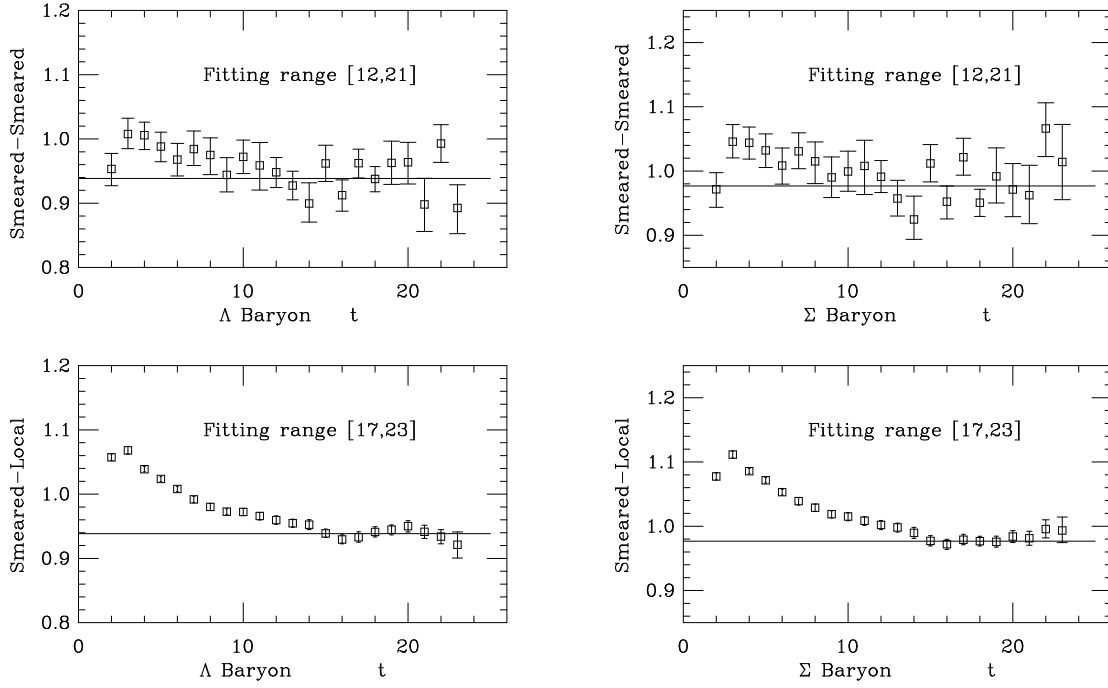


Figure 1: *Effective masses for the Λ and Σ baryons. We show typical plots, corresponding to $\kappa_h = 0.129$ and $\kappa_{l1} = \kappa_{l2} = 0.14144$. The straight lines are our best fits, which agree for SL and SS correlators starting from $t_{\min} = 17$ onwards.*

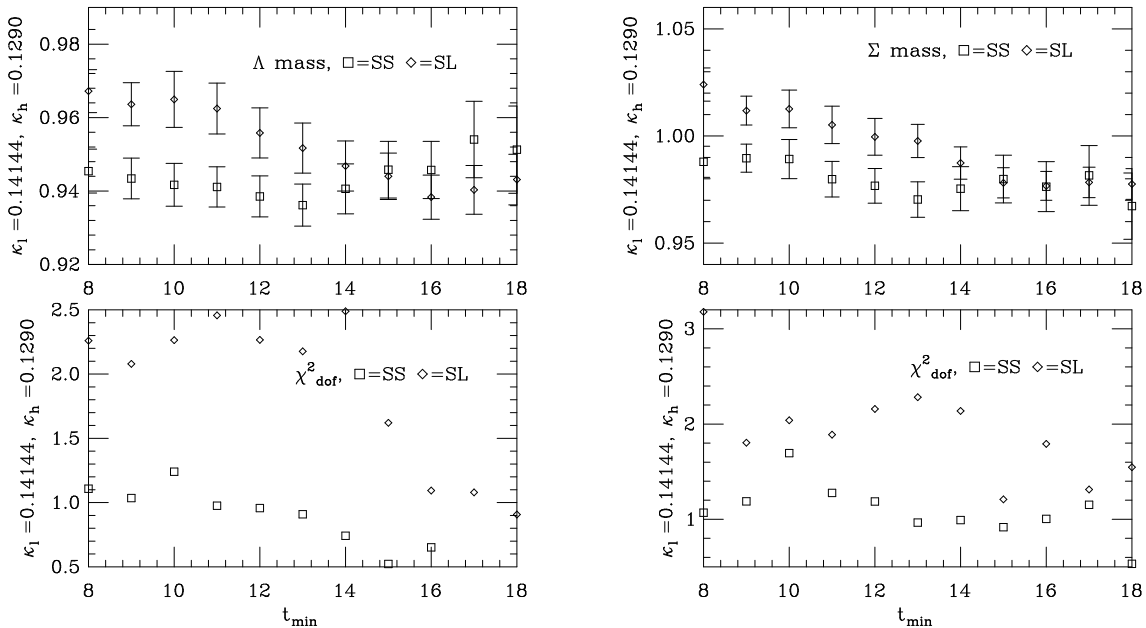


Figure 2: *Masses and χ^2/dof obtained from a sliding window analysis for the Λ and the Σ baryon correlators.*

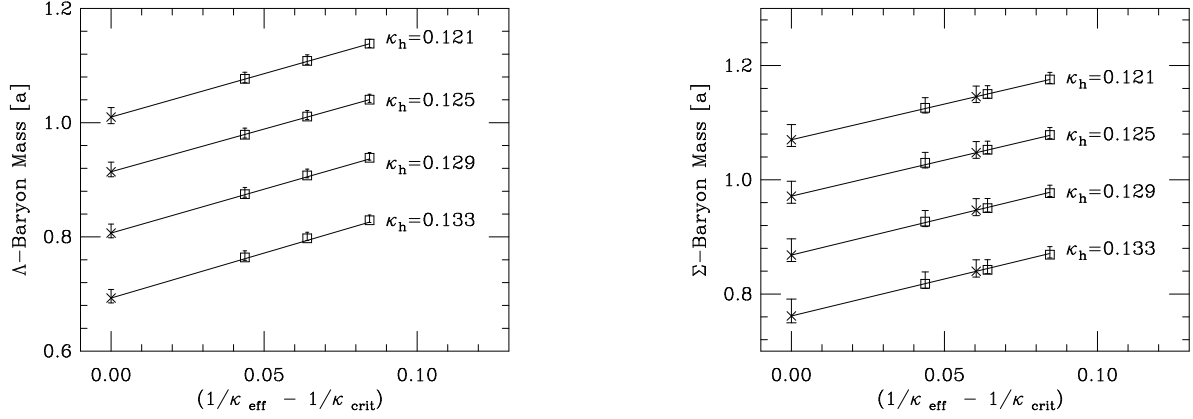


Figure 3: *The chiral behaviour of the Λ and Σ masses. The boxes denote data at our three light-quark masses; the crosses denote the extrapolation of our results to the chiral limit and the strange-quark mass.*

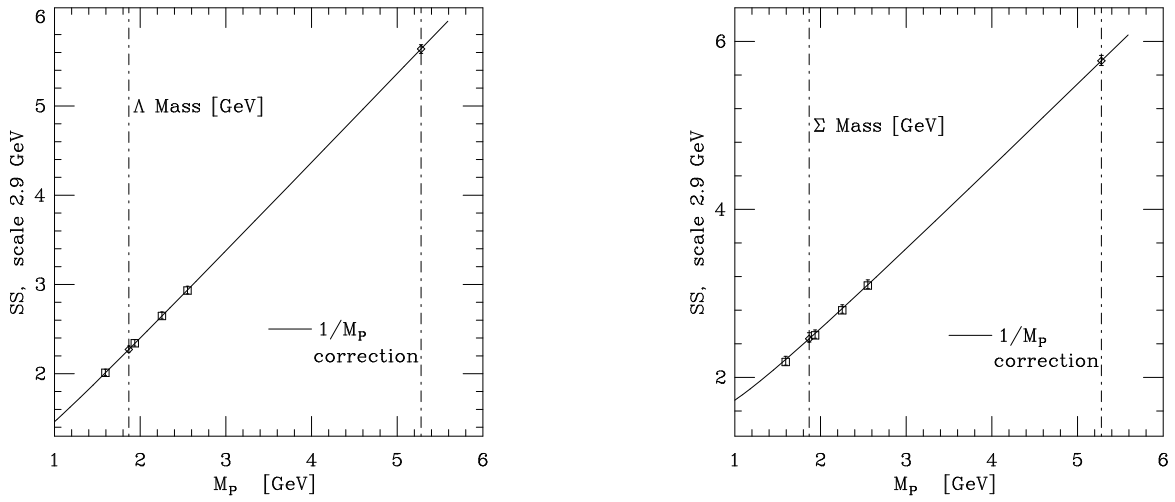


Figure 4: *Extrapolation of the Λ and Σ baryon masses. In the figures both the linear extrapolation and that obtained taking into account $O(1/M_P)$ correction are shown. The diamonds and crosses correspond to the extrapolations to the charm mass and beauty mass respectively.*

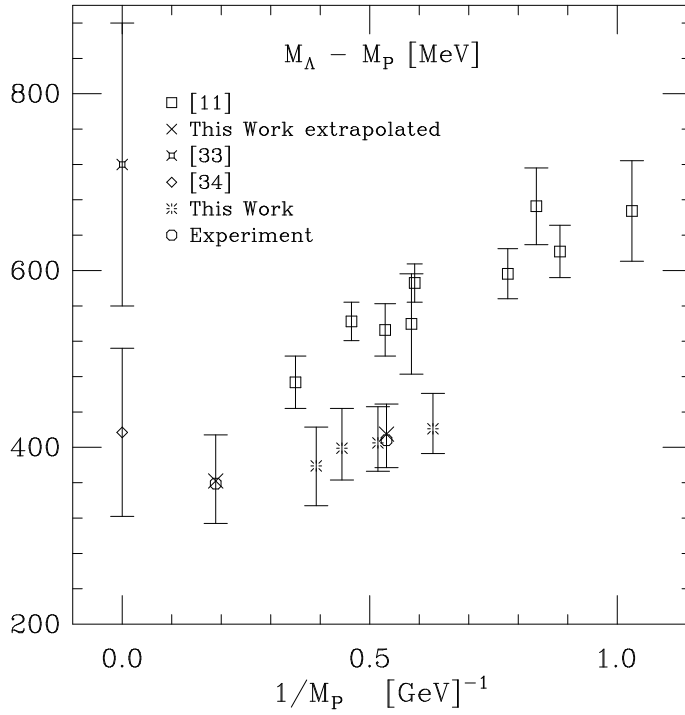


Figure 5: $M_\Lambda - M_P$ splitting: comparison of the values obtained by different groups and using different fermion actions. The estimates are also compared with the experimental numbers.

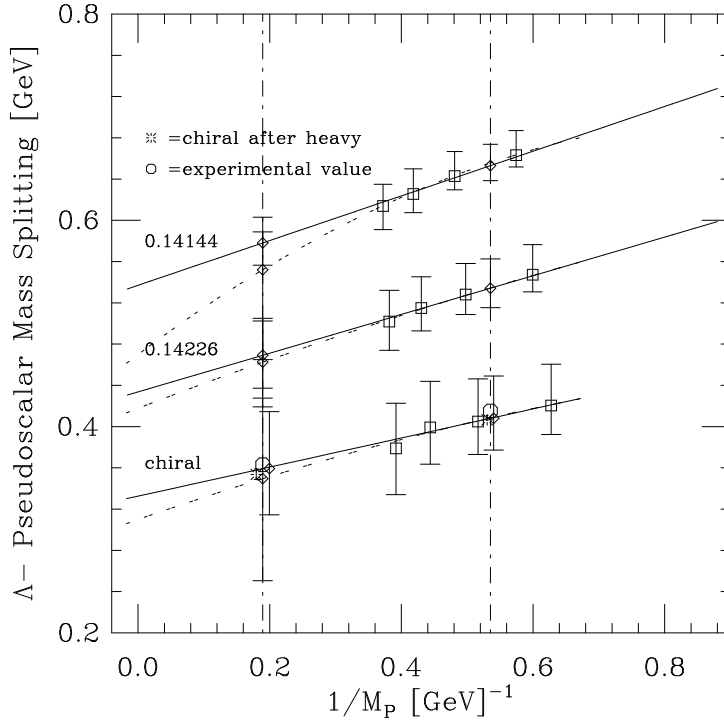


Figure 6: $M_\Lambda - M_P$ splitting as obtained adopting the two procedures A and B. The solid lines correspond to the linear extrapolation in the inverse pseudoscalar mass and the dotted line is the same extrapolation modelled with a quadratic dependence. In the plot, the light κ values are also indicated. The results, which are consistent between both methods, are compared with the experimental values. The vertical dotted lines indicate $1/M_D$ and $1/M_B$.

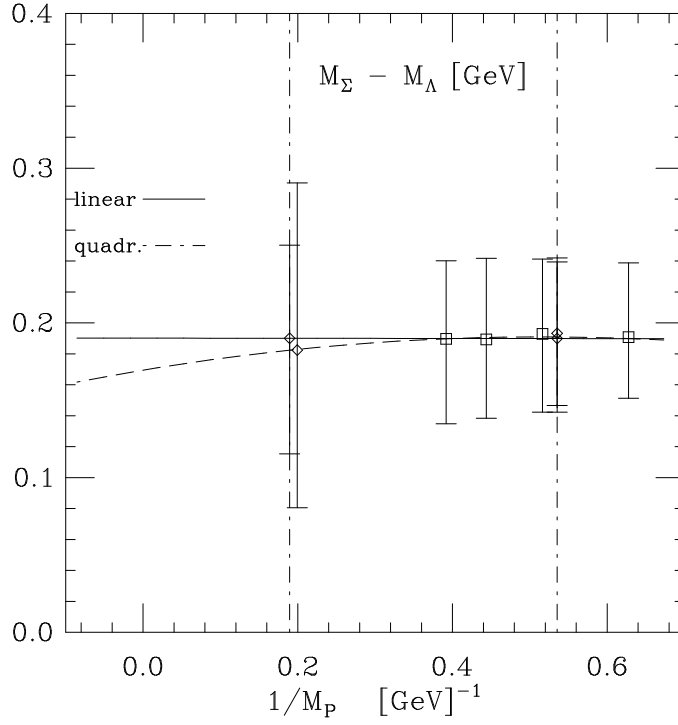


Figure 7: $M_\Sigma - M_\Lambda$ as a function of $1/M_P$. The linear and the quadratic extrapolation are shown. The vertical dotted lines indicate $1/M_D$ and $1/M_B$, respectively.

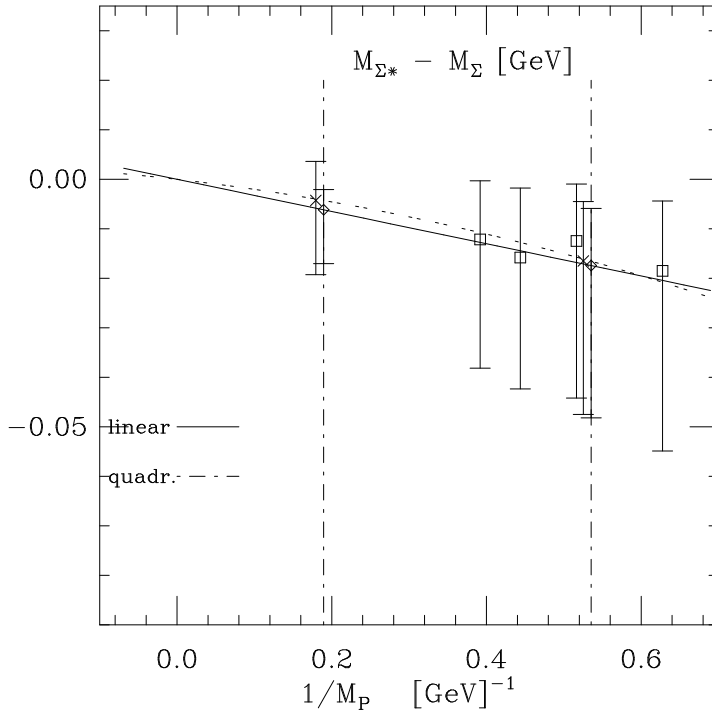


Figure 8: $M_{\Sigma^*} - M_\Sigma$ splitting computed from the mass difference, together with linear and quadratic extrapolations. The vertical dotted lines indicate $1/M_D$ and $1/M_B$.

